This is a repository copy of *Death from drought in tropical forests is triggered by hydraulics not carbon starvation*.

Article:

1 **Death from drought in tropical forests is triggered by hydraulics not carbon starvation**

2 Rowland, L[1]., da Costa, A. C. L.[2], Galbraith, D. R[3]., Oliveira. R. S.[4], Binks, O. J.[1], Oliveira,

3 A. A. R.[2], Pullen, A. M[5]., Doughty, C. E.[6], Metcalfe, D. B.[7], Vasconcelos, S. S.[8], Ferreira, L.

4 V.[9], Malhi, Y.[6], Grace, J.[1], Mencuccini, M.[1,10] and Meir, P.[1,11]

5

6 [1] School of GeoSciences, University of Edinburgh, Edinburgh, UK

7 [2] Centro de Geosciências, Universidade Federal do Pará, Belém, Brasil

8 [3] School of Geography, University of Leeds, Leeds, UK

9 [4] Instituto de Biologia, UNICAMP, Campinas, Brasil

10 [5] The University of Cambridge, Cambridge, UK

11 [6] Environmental Change Institute, The University of Oxford, Oxford, UK

12 [7] Department of Physical Geography and Ecosystem Science, Lund University, Lund, Sweden

13 [8] EMBRAPA Amazônia Oriental, Belém, Brasil

14 [9] Museu Paraense Emílio Goeldi, Belém, Brasil

15 [10] ICREA at CREAF, 08193 Cerdanyola del Vallés, Spain

16 [11] Research School of Biology, Australian National University, Canberra, Australia

17

18 Drought threatens tropical rainforests over seasonal to decadal timescales[1-4], but the drivers

19 of tree mortality following drought remain poorly understood[5,6]. It has been suggested that

20 reduced availability of non-structural carbohydrates (NSC) critically increases mortality risk

21 through insufficient carbon supply to metabolism ('carbon starvation')[7,8]. However little is

22 known about how NSC stores are affected by drought, especially over the long term, and

23 whether they are more important than hydraulic processes in determining drought-induced

24 mortality. Using data from the world's longest-running experimental drought study in tropical

25 rainforest (in the Brazilian Amazon), we test whether carbon starvation or deterioration of the

26 water-conducting pathways from soil to leaf trigger tree mortality. Biomass loss from

27 mortality in the experimentally-droughted forest increased substantially after >10 years of

28 reduced soil moisture availability. The mortality signal was dominated by the death of large

29 trees, which were at a much greater risk of hydraulic deterioration than smaller trees.

30 However, we find no evidence that the droughted trees suffered carbon starvation, as their

31 NSC concentrations were similar to those of un-droughted trees, and growth rates did not

32 decline in either living or dying individuals. Our results indicate that hydraulics, rather than

33 carbon starvation, triggers tree death from drought in tropical rainforest.

34

35 Drought-response observations from both field-scale experiments and natural droughts have

36 demonstrated increased mortality over the short-term (1-3 years), with notably higher

37 vulnerability for some taxa, and for larger trees[6,9,10]. After several years of drought,

38 recovering growth rates in smaller trees, dbh (diameter at breast height) <40 cm, and reduced

39 mortality have been recorded at different locations[6,11,12]. However, the long-term (>10 yr)

40 sensitivity of tropical forests to predicted prolonged and repeated water deficit[1-3] and the

41 physiological mechanisms influencing this are poorly understood. Through-fall exclusion

42 (TFE) studies, that create soil moisture deficit by the exclusion of a fraction of incoming

43 rainfall, provide the only current means to assess the long-term response in mechanistic

44 detail[5,13].

45 Trees experiencing drought stress are thought to die from direct physiological failure and/or

46 from injury and biotic attack associated with a decline in physiological vigour[14]. A global

47 effort to identify the relevant physiological mechanisms triggering death and thus to improve

48 predictions of forest tree mortality has focussed on the twin possibilities of: (i) failure to

49   supply sufficient carbon substrate to metabolism following drought-related reductions in

50   photosynthesis and increased use of NSC, theoretically leading to carbon starvation; and (ii)

51   deterioration of the water-conducting xylem tissue, causing a rapid or gradual failure of key

52   dependent processes (e.g., gas exchange, photosynthesis, phloem transport), and potentially

53   leading to tissue desiccation[14,15], ultimately leading to mortality. Despite recent intensive

54   research, it is unclear how important these two mechanisms are in different biomes and how,

55   or whether, to model them[16].

56   Since 2002 a 50% TFE treatment has been implemented at a 1 ha-scale drought experiment in

57   old-growth forest at Caxiuanã National Forest Reserve, Pará State, Brazil[6,12], to simulate

58   possible rainfall reductions predicted to occur in parts of Amazonia by 2100[1]. Mortality

59   surveys, recruitment and growth rates of all trees ≥10 cm dbh, have been monitored through

60   the experimental period (see Methods). Recently, seasonal data on NSC concentrations were

61   measured on leaves, branches and stems of 41 trees (20 trees on the control, 21 trees on the

62   TFE) of the most common genera in the experiment (Extended Data Table 1). Xylem

63   vulnerability curves were also performed on the branches of these trees (see Methods). Here,

64   we synthesise these data to test whether long-term soil moisture deficit alters NSC storage

65   and use in tropical rainforest trees, and if this, or hydraulic processes, are most strongly

66   associated with increased mortality rates.

67   By 2014, following 13 years of the TFE treatment, cumulative biomass loss through mortality

68   was 41.0±2.7% relative to pre-treatment values (Fig. 1a), and the rate of loss had increased

69   substantially since the previous reported value of 17.2±0.8%, after 7 years of TFE[6].

70   Accelerating biomass loss and failure to recover substantially, or to reach a new

71   equilibrium[13], has led to a committed flux to the atmosphere from decomposing necromass of

72   101.9 ± 19.1 Mg C ha^{-1} (Fig. 1a). This biomass loss has been driven by elevated mortality in

73 the largest trees (Fig. 1b), as previously observed over shorter timescales[6], and has created a

74 canopy that has had a persistently lower average leaf area index during 2010-2014

75 (12.0±1.2% lower; Extended data Fig. 1).

76 Remarkably, individual tree growth rates for the four years prior to death showed no

77 significant reduction in either the TFE or control plots (Fig. 2a), indicating that growth is

78 prioritised to the point of death irrespective of the soil moisture deficit treatment. From 2008,

79 tree growth in every wet season (January-June) on the TFE treatment relative to the control

80 was significantly elevated ($P<0.05$) in the small and medium trees (up to 4.6±0.2 times

81 higher in small trees, and 2.9±0.2 times higher in medium trees), and maintained in the

82 largest trees (10-20 cm, 20-40 cm and >40 cm dbh, respectively; Fig. 2b-d). Elevated wet

83 season growth occurred despite 0.1-0.9 MPa reduction in average soil water potential (Ψ_s) at

84 depths of 0-4 m on the TFE and a loss of seasonality in Ψ_s (Extended Data Fig. 2). Increased

85 growth in the small trees occurred from 2008 onwards, following earlier substantial mortality

86 of large trees (Fig. 1), which generated canopy gaps. Increased light availability to smaller

87 trees, and presumably reduced below-ground competition for water and nutrients, allowed

88 competitive release of trees on the TFE[8], and elevated growth rates. Competitive release on

89 the TFE implies that, following 13 years of drought-stress, photosynthetic production is

90 sufficient not only to maintain growth in the largest trees (Fig. 2d), but to increase growth in

91 trees <40 cm dbh (Fig. 2b-c). This response would not be possible if the majority of trees

92 were severely carbon limited, unless very considerable long-term (or renewed) carbon

93 resources were being drawn upon.

94 Prioritisation of growth under drought in the TFE is consistent with recent observations

95 following short-term drought in Amazonia[7]. However, the maintenance of NSC

96 concentrations in the TFE treatment suggests that the prioritisation of growth during drought

97   does not occur at the expense of depleted carbon stores, as previously hypothesised[7]. Neither

98   the concentrations of soluble sugar (carbon immediately available to metabolism) nor starch

99   (stored carbon which can be converted to sugars) were significantly depleted in stem, leaf and

100 branch tissue from the TFE, relative to control (Fig. 3). The seasonal changes in both sugar

101 and starch concentrations, which varied by 50-90%, were much larger than any differences

102 associated with the TFE treatment (Fig. 3). Despite 13 years of severely reduced soil moisture

103 availability, the seasonal cycle and use of NSCs was unaltered, implying that the sampled

104 trees did not draw significantly upon their NSC reserves to buffer against the long-term

105 effects of soil moisture deficit. Large changes in carbon allocation from roots and leaves to

106 maintain stem growth during drought[17] have not been reported on the TFE[12]. Similarly no

107 drought-induced reductions in photosynthetic capacity occurred on the TFE[18], although how

108 total canopy productivity is affected remains uncertain. Considering this and additional

109 evidence of no increase in herbivore attack on the TFE (Extended Data Fig. 3), our results

110 suggest progressive carbon starvation and biotic foliar consumption are not important drivers

111 of the mortality patterns observed in the TFE forest following extended severe soil moisture

112 deficit (>10 years).

113 Deterioration of the water transport system in the xylem tissues following drought can also

114 lead to death[17,19]. The vulnerability of the xylem to drought is described by a vulnerability

115 curve[20], which relates water potential in xylem conduits to loss of hydraulic conductivity

116 because of occlusions by gas emboli. The water potential at which 50% loss of xylem

117 conductivity occurs ($P_{50,}$ MPa) is a commonly used index of embolism resistance[20]. We

118 determined xylem P_{50} for the trees on the control and TFE plots, with tree dbh ranging from

119 15 to 48 cm. A highly significant decrease in P_{50} with dbh was found across TFE and control

120 (Extended Data table 3, $P<0.01$). As dbh increased from 15 to 48 cm there was a 1.3±0.2

121 MPa reduction in the P_{50} value, with significant genus-to-genus differences (Fig.4). Leaf

122   water potential (Ψ_l) could only be measured during limited sampling campaigns (2-3 days)

123   that were characterised by low vapour pressure deficit (VPD, 54-59% of peak dry season

124   values) and unseasonal rainfall in the preceding days. Differences between treatment and

125   control Ψ_l were not detected. Mean midday Ψ_l recorded across all the trees together with the

126   vulnerability curves determined for each genus were used to predict the percentage loss of

127   xylem conductivity (PLC) with dbh. Values of PLC at mean Ψ_l increased with dbh, with the

128   largest diameter trees predicted to have reductions in conductive capacity of about 80% in

129   some genera, indicating significant vulnerability to hydraulic deterioration (inset of Fig. 4).

130   Given no evidence of carbon starvation and similar Ψ_l across plots in the sample dates, why

131   did many more trees die in TFE than control? The lack of treatment differences in Ψ_l

132   contrasts starkly with the long-term records of lower Ψ_s (Extended Data Fig. 2). The lack of

133   difference in midday Ψ_l could have been caused by sampling constraints or by isohydric

134   behaviour. We found evidence of non-isohydric behaviour in our diurnal Ψ_l measurements

135   (Extended Data Fig. 4), with overall strong linear declines in Ψ_l observed with increasing

136   VPD on the control (R^2=0.18, P<0.01) and in particular on the TFE (R^2=0.33, P<0.01).

137   Consequently limited sampling is the most likely cause of equal Ψ_l between the two plots,

138   with TFE trees likely having more negative Ψ_l and lower hydraulic conductance during VPD

139   maxima in the dry season. Reduced carbon uptake because of stomatal closure in some TFE

140   trees is possible[21], but is unlikely to have caused carbon starvation considering growth rates

141   were maintained or elevated on the TFE (Fig. 2) and radial growth should decline prior to

142   photosynthesis in drought conditions[22]. Even with an isohydric response, trees on the TFE

143   would still be likely to suffer greater hydraulic deterioration caused by greater PLC in the

144   roots and main stem. Strongly reduced Ψ_s on the TFE (Extended Data Fig. 2) and significant

145   hydraulic vulnerability of the tall trees are consistent with the hypothesis of hydraulic

146   deterioration as the most likely trigger of greater mortality, particularly in the largest trees, as

147   observed. Why the xylem tissue of larger trees is more vulnerable to embolism deserves

148   further study. Taller trees are predisposed to greater hydraulic stress, from elevated

149   atmospheric demand and longer hydraulic path lengths[23]. As the canopies are exposed to

150   rainfall in the TFE, smaller trees could avoid hydraulic deterioration through leaf water

151   uptake[24-26], but this may not be sufficient to save the largest trees, which we hypothesise are

152   forced to maintain their high growth rates until death to continually replace dysfunctional

153   xylem.

154   Following decadal-scale soil moisture depletion, our results suggest tropical rainforests will

155   experience accelerating biomass loss and a likely transition to a lower statured, lower

156   biomass forest state, due to substantially elevated mortality of the largest trees. This mortality

157   is most likely triggered by hydraulic processes, which lead to hydraulic deterioration and

158   subsequent, potentially rapid, limitations in carbon uptake[21], instead of being caused directly

159   by gradual carbon starvation. Under natural drought these forests may be under greater risk

160   than from experimental drought, as severe soil moisture deficit is combined with low

161   humidity and high air temperature increasing hydraulic demand. Improved prediction of the

162   sensitivity of tropical tree mortality to drought should therefore focus on improved model

163   simulation of plant hydraulics and modelling environmental controls on growth[27,22]. Decadal-

164   scale ecological data such as these are rare, but they are invaluable for testing and improving

165   predictions from vegetation models over timescales that are relevant to climate change[28].

166   They also underpin the long-term environmental policy needed to manage the natural capital

167   that is embedded in tropical rainforests.

168

Author contributions

LR, PM, ALDC and MM designed and implemented the research. PM conceived and led the experiment and this study. LR led recent measurements; all authors contributed to data collection, led by ALDC. LR analysed the data with MM, PM, OB and AMP. LR wrote the paper with PM and MM, with contributions from all authors.

189   **References**

190

191   1   Christensen, J. H. *et al.* in *Climate Change 2013: The Physical Science Basis.*

192   *Contribution of Working Group I to the Fifth Assessment Report of the*

193   *Intergovernmental Panel on Climate Change*   (ed T.F. Stocker, Qin, D. , Plattner,

194   G.-K., Tignor, M., Allen, S.K., Boschung, J., Nauels, A., Xia, Y., Bex, V., and

195   Midgley, P.M. (eds.)) (Cambridge University Press, 2013).

196   2   Mora, C. *et al.* The projected timing of climate departure from recent variability.

197   *Nature* 502, 183-187, doi:Doi 10.1038/Nature12540 (2013).

198   3   Reichstein, M. *et al.* Climate extremes and the carbon cycle. *Nature* 500, 287-295,

199   doi:Doi 10.1038/Nature12350 (2013).

200   4   Boisier, J. P., Ciais, P., Ducharne, A. & Guimberteau, M. Projected strengthening of

201   Amazonian dry season by constrained climate model simulations. *Nature Clim.*

202   *Change* 5, 656-660, doi:10.1038/nclimate2658 (2015).

203   5   Hartmann, H., Adams, H. D., Anderegg, W. R. L., Jansen, S. and Zeppel, M. J. B.

204   Research frontiers in drought-induced tree mortality: crossing scales and disciplines.

205   *New Phytol*, 965-969, doi:doi: 10.1111/nph.13246 (2015).

206   6   da Costa, A. C. L. *et al.* Effect of 7 yr of experimental drought on vegetation

207   dynamics and biomass storage of an eastern Amazonian rainforest. *New Phytol* 187,

208   579-591, doi:DOI 10.1111/j.1469-8137.2010.03309.x (2010).

209   7   Doughty, C. E. *et al.* Drought impact on forest carbon dynamics and fluxes in

210   Amazonia. *Nature* 519, 78-U140, doi:Doi 10.1038/Nature14213 (2015).

211   8   O'Brien, M. J., Leuzinger, S., Philipson, C. D., Tay, J. & Hector, A. Drought survival

212   of tropical tree seedlings enhanced by non-structural carbohydrate levels. *Nat Clim*

213   *Change* 4, 710-714, doi:Doi 10.1038/Nclimate2281 (2014).

214   9   Nepstad, D. C., Tohver, I. M., Ray, D., Moutinho, P. & Cardinot, G. Mortality of

215   large trees and lianas following experimental drought in an amazon forest. *Ecology*

216   88, 2259-2269, doi:Doi 10.1890/06-1046.1 (2007).

217   10   Phillips, O. L. *et al.* Drought Sensitivity of the Amazon Rainforest. *Science* 323,

218   1344-1347, doi:DOI 10.1126/science.1164033 (2009).

219   11   Brando, P. M. *et al.* Drought effects on litterfall, wood production and belowground

220   carbon cycling in an Amazon forest: results of a throughfall reduction experiment.

221   *Philos T R Soc B* 363, 1839-1848, doi:DOI 10.1098/rstb.2007.0031 (2008).

222   12   da Costa, A. C. L. *et al.* Ecosystem respiration and net primary productivity after 8-10

223   years of experimental through-fall reduction in an eastern Amazon forest. *Plant Ecol*

224   *Divers* 7, 7-24, doi:Doi 10.1080/17550874.2013.798366 (2014).

225   13   Meir, P. *et al.* Threshold responses to soil moisture deficit by trees and soil in tropical

226   rain forests: insights from field experiments. *Bioscience, in press* (2015).

227   14   McDowell, N. G. *et al.* The interdependence of mechanisms underlying climate-

228   driven vegetation mortality. *Trends Ecol Evol* 26, 523-532, doi:DOI

229   10.1016/j.tree.2011.06.003 (2011).

230   15   Thomas, H. Senescence, ageing and death of the whole plant. *New Phytol* 197, 696-

231   711, doi:Doi 10.1111/Nph.12047 (2013).

232   16   Meir, P., Mencuccini, M. & Dewar, R. C. Drought-related tree mortality: addressing

233   the gaps in understanding and prediction. *New Phytol*, n/a-n/a, doi:10.1111/nph.13382

234   (2015).

235   17   Anderegg, W. R. L. *et al.* Drought's legacy: multiyear hydraulic deterioration

236   underlies widespread aspen forest die-off and portends increased future risk. *Global*

237   *Change Biol* 19, 1188-1196, doi:Doi 10.1111/Gcb.12100 (2013).

238   18   Rowland, L. *et al.* After more than a decade of soil moisture deficit, tropical rainforest

239   trees maintain photosynthetic capacity, despite increased leaf respiration. *Global*

240   *Change Biol* (2015), doi: Doi 10.1111/gcb.13035.

241   19   Anderegg, W. R. *et al.* The roles of hydraulic and carbon stress in a widespread

242   climate-induced forest die-off. *Proc Natl Acad Sci U S A* 109, 233-237,

243   doi:10.1073/pnas.1107891109 (2012).

244   20   Choat, B. *et al.* Global convergence in the vulnerability of forests to drought. *Nature*

245   491, 752-755, doi:10.1038/nature11688 (2012).

246   21   Sala, A., Woodruff, D. R. & Meinzer, F. C. Carbon dynamics in trees: feast or famine?

247   Tree Physiol 32, 764-775, doi:10.1093/treephys/tpr143 (2012).

248   22   Körner, C. Carbon limitation in trees. *J Ecol* 91, 4-17, doi:DOI 10.1046/j.1365-

249   2745.2003.00742.x (2003).

250   23   Mencuccini, M. *et al.* Size-mediated ageing reduces vigour in trees. *Ecol Lett* 8, 1183-

251   1190, doi:DOI 10.1111/j.1461-0248.2005.00819.x (2005).

252   24   Burkhardt, J., Basi, S., Pariyar, S. & Hunsche, M. Stomatal penetration by aqueous

253   solutions - an update involving leaf surface particles. *New Phytol* 196, 774-787,

254   doi:DOI 10.1111/j.1469-8137.2012.04307.x (2012).

255   25   Yates, D. J. & Hutley, L. B. Foliar uptake of water by wet leaves of Sloanea-Woollsii,

256   an australian subtropical rain-forest tree. *Aust J Bot* 43, 157-167, doi:Doi

257   10.1071/Bt9950157 (1995).

258   26   Eller, C. B., Lima, A. L. & Oliveira, R. S. Foliar uptake of fog water and transport

259   belowground alleviates drought effects in the cloud forest tree species, Drimys

260   brasiliensis (Winteraceae). *New Phytol* 199, 151-162, doi:Doi 10.1111/Nph.12248

261   (2013).

262   27   Fatichi, S., Leuzinger, S. & Korner, C. Moving beyond photosynthesis: from carbon

263   source to sink-driven vegetation modeling. *New Phytol* 201, 1086-1095, doi:Doi

264   10.1111/Nph.12614 (2014).

265   28   Leuzinger, S. *et al.* Do global change experiments overestimate impacts on terrestrial

266   ecosystems? *Trends Ecol Evol* 26, 236-241, doi:DOI 10.1016/j.tree.2011.02.011

267   (2011).

268

269

270

Figure Legends

Fig. 1| Changes in biomass and mortality rates. a. Biomass on the control and TFE plot

from 2002-2014 (Mg C ha^{-1} yr^{-1}). Error bars show the s.e.m. calculated from 12 estimates of

biomass, accounting for uncertainty in wood density and allometric equations (see Methods).

b. Mortality rate (% stems year^{-1}) calculated separately for trees of 10-20 cm dbh, 20-40 cm

dbh and >40 cm dbh on the control (black) and TFE (grey). The genus at date of death for

each tree used in the mortality rate calculations is shown in Extended data Table 2.

Fig. 2| Tree growth of living and dead trees. a. Average annual stem increment in the four

years prior to death for all trees which died on the control (*n*=35) and TFE (*n*=60) from 2005

onwards. Growth rates are normalised by the growth in year 0, the year in which the tree

died. b-d. Stem increment for small (a. 10-20 cm dbh), medium (b. 20-40 cm dbh) and large

(c. >40 cm dbh) trees on the control and TFE plot from 2005 to 2014. Values for b-d are

normalised by the maximum increment on the control plot. Error bars show the s.e.m.

Fig. 3| Leaf, branch and stem NSC concentrations. Percentage values for soluble sugars

(a.) and starch (b.) in dried biomass of leaves, branches and stems on the control and TFE for

late dry season (November 2013), mid wet season (March 2014) and in the wet-to-dry

transition (June 2014) for trees on the control (*n*=20) and TFE (*n*=21). Error bars show s.e.m.

and * indicates a significant difference at $P < 0.05$ using the Wilcoxon test. June 2014 has

significantly elevated sugar values on the TFE plot, however the absolute values for sugar

concentration are very low, and the absolute differences are very small.

Figure 4| Xylem vulnerability to embolism and predicted loss of xylem hydraulic

conductivity as a function of tree diameter (dbh). A general linear model was employed to

test for the effects of genus and tree dbh on the estimates of xylem P_{50} obtained for each

species (*n*=37 trees in total). The dashed lines give the predicted regressions for each of the

295 six genera, whereas the bold black line gives the overall mean regression line across all

296 species (The adjusted R^2 in the figure refers to the overall model, while the P value refers to

297 the significance of tree dbh). The insert shows the changes in predicted losses of hydraulic

298 conductivity (PLC) as a function of tree size. In the main graph, each genus is represented

299 with a different symbol and/or colour, as detailed in the legend. In the inset, the bold lines

300 represent the average prediction for the most vulnerable genus (red: *Pouteria*) and for the

301 most resistant one (blue: *Licania*) to drought induced embolism, with the shaded areas (pink,

302 light blue) giving the respective 95% confidence intervals.

303

304 **Extended data Figure 1| Leaf area index change:** leaf area index (LAI; m^2 leaf area m^{-2}

305 ground area) for the period of 2001-2014 on the control (black, solid) and TFE (grey, dashed)

306 plots. Error bars show the s.e.m. associated with LAI calculation (see Methods).

307 **Extended Data Fig. 2| Seasonal soil water potential:** average soil water potential (- MPa)

308 in the control and TFE during dry season (July-December) and wet season (January-June),

309 calculated form monthly average volumetric soil moisture content data, collected from 2008-

310 2014, using sensors installed 0, 0.5, 1, 2.5 and 4 m below the surface and the necessary van

311 Genuchten parameters previously calculated from soil hydraulics measurements at this site

312 (see Methods). They are averaged from hourly data collected from 2008-2011 and error bars

313 show s.e.m.

314 **Extended data Figure 3| Leaf herbivory comparison:** average percentage loss of leaf area

315 from herbivore attack calculated from 9770 leaves collected in litter-traps on the control and

316 TFE plot from 2010-2014. Error bars show s.e.m. A separate analysis of herbivore attack on

317 13,694 top-canopy living leaves from branches of the 41 trees used for the P_{50} analysis

318 support these results, also showing no significant differences in percentage herbivory

319 between the control and the TFE (data not shown).

320 **Extended Data Figure 4| Diurnal patterns of Ψ_l**: diurnal Ψ_l measured every 2 hours from

321 6.00 until 18.00 in dry season on trees accessible from the walk up tower. Each box shows

322 the diurnal Ψ_l against diurnal air vapour pressure deficit (VPD) from one of seven trees

323 accessible on the control (C), or one of four trees accessible on the TFE. Note a majority of

324 trees demonstrate some a negative relationship with VPD. Combined separately for each plot,

325 a significant negative linear relationship is observed between Ψ_l and VPD on the control

326 (R^2=0.18, P=0.002) and even more strongly on the TFE (R^2=0.33, P=0.001).

327

328

329

Methods

Site: The through-fall exclusion (TFE) experiment is located in the Caxiuanã National Forest

Reserve in the eastern Amazon (1°43'S, 51°27W), ~400 km west of the nearest city, Belém,

State of Pará, Brazil. The experiment is located in *terra firme* forest, on yellow oxisol soils

which are 75-83 % sand, 12-19 % clay and 6-10 % silt[29]. The site is 15 m above sea level, has

a mean annual rainfall between 2000-2500 mm and a pronounced dry season between June

and November[2].

The experimental site has two 1 ha plots: the TFE, over which plastic panels and gutters have

been placed at a height of 1-2 m, and which exclude 50% of the incident rainfall; and a

corresponding control plot, <50 m from the TFE, on which there has been no manipulation of

incident rainfall. The TFE was trenched to between 1-2 m to remove the effect of through-

flow of soil water; and to control for any temporary damage to roots from the trenching, the

control plot was also trenched to the same depth. The TFE treatment has been installed and

running continuously since January 2002 to the present, except for a 1 week period in

November 2002 (full removal), a month period during the dry season in November 2014

(sequential removal of all panel) and during 2004 (30% removal).

Soil Moisture Data: In both the control and TFE plots there are soil access pits in which

volumetric soil water content sensors (CS616, Campbell Scientific, Logan, USA) located at

depths of 0, 0.5, 1, 2.5 and 4 m, monitor soil moisture every hour (*cf.* Fisher et al.[30], for full

methodology). New data presented here are from March 2008 - December 2014, averaged

into monthly values. Due to equipment failure, some soil moisture data are missing for

August and December 2013, for 2008 and 2010 on the control plot, and for November and

December 2013 on the TFE plot. Volumetric soil water content was converted in to soil water

353   potential (Ψ_s) using the necessary van Genuchten parameters previously calculated by Fisher

354   et al.[31] based on soil hydraulics measurements at this site.

355   *Biomass data:* Trees ≥10 cm diameter at breast height (dbh) on both the control and the TFE

356   plots were tagged and identified to species level in September 2000. Diameters were

357   measured on these trees at 1.3 m, unless buttress roots were present, in which case the

358   measurement was made above the buttressing. Individuals on the plots were re-censused at

359   varying intervals from January 2001, until November 2014. During each census the trees

360   were also assessed to be either dead or alive. A tree was considered dead if leaflessness was

361   accompanied by a persistent zero or negative stem increment, and/or the tree had snapped or

362   fallen to the ground. Recruitment of new trees into the ≥10 cm dbh size class was enumerated

363   in 2005, 2009 and 2014.

364   Trees in the 10 x 10 m subplots adjacent to the trenches were excluded from our biomass and

365   growth rate analysis to eliminate possible effects of changes in mortality resulting from root

366   damage[2]. Consequently, 369 trees on the control and 358 trees on the TFE, each in 0.64 ha

367   were analysed and the biomass scaled to 1 ha. Following da Costa et al. (2010)[6] trees were

368   grouped into small (10-20 cm dbh) and medium (20-40 cm dbh) and large (>40 cm dbh) size

369   classes.

370   Biomass was calculated using the Chave et al.[32] equation which uses diameter, wood density

371   and environmental predictors. A mean and standard deviation of wood density for each tree

372   was calculated from data in the global wood density database[33,34] and from Patiño et al.[35].

373   Multiple estimates of wood density at the species, genus and family level were used to

374   calculate standard deviations on our wood density estimates. Of all the trees on both plots, 68

375   % had values for wood density at species level, 18 % at genus level and 3 % at family level;

376   11 % of trees were not identified and were given a plot level average wood density with an

377   associated standard deviation. A standard error on our biomass estimations was calculated,

378   which accounted for the error associated with wood density estimation and variations in

379   commonly used allometric equations. Twelve calculations were used to calculate the error on

380   our biomass values; these 12 biomass estimates were from combinations of four biomass

381   equations: Chave et al.[32] and Chave et al.[36] both with and without height and three wood

382   density estimates: mean wood density and mean wood density ± one standard deviation. The

383   allometric equations selected represent one of the most commonly used biomass equations for

384   Amazonia[36] (with and without height as a predictor variable) and the most recent and most

385   comprehensive biomass equations for our study area[32] (with and without height as a predictor

386   variable). Measurements of height were not available and were calculated from an equation

387   developed specifically for the region of the Amazon in which our plots are located[37].

388   Mortality rate was calculated according to da Costa et al. (2010)[6] and separately for trees of

389   10-20 cm dbh, 20-40 cm dbh and >40 cm dbh on the TFE and control plot.

390   *Seasonal growth data:* Dendrometers were installed at just above or below the point of dbh

391   measurement on all trees ≥10 cm dbh[38]. Circumference measurements from the dendrometer

392   bands were made monthly to tri-monthly from January 2005 to November 2014, with the

393   exception of a six month gap from July 2007 and January 2013. Seasonal shrinkage was

394   calculated by taking the average growth rate of 19 trees on the control and TFE plots which

395   experienced no overall growth, but demonstrated a seasonal pattern of shrinkage and

396   expansion. Tropical trees can experience net diameter shrinkage in the dry season, due to a

397   lack of growth, accompanied by reduced water content of stem tissues, with subsequent

398   swelling when tissues are rehydrated in the wet season[39]. An average pattern of shrinkage and

399   expansion was therefore subtracted from all trees to ensure that dry season growth was not

400   under-estimated and wet season growth over-estimated. Dendrometer increments were

401   filtered to remove the growth spikes from measurement errors following Rowland et al.

402   (2014)[39]. Subsequent to this procedure, gap-filling was done using linear interpolation[39]; on

403   the control and TFE plot 16 % and 17 % of the data were gap-filled respectively. Growth

404   rates per day calculated from the dendrometer measurements were averaged into three

405   monthly periods to give continuous tri-monthly growth rates from 2005-2014. When trees in

406   the 10 x 10 m subplots adjacent to the trenches, and trees with poor quality dendrometer

407   measurements throughout the 10 year study period for growth were excluded, 316 and 310

408   trees on the control and TFE plot remained, respectively. All growth and mortality analyses

409   were done using the R statistical package (version 3.1.2). Tests for significance were

410   performed using Wilcoxon signed-rank test.

411   *Non Structural Carbohydrate (NSC) analysis*. Using samples cut by a tree climber from fully

412   sunlit branches, three leaves and a branch sample of ~ 8-10 mm diameter were taken from 20

413   trees on the control plot and 21 trees on the TFE plot in November 2013, March 2014 and

414   June 2015. The numbers and species of the trees selected for analysis are shown in Extended

415   Data Table 1. The selected trees were all >10 cm dbh and represented the most common

416   genera existing on both plots[2]; samples were not taken from the external 10 x 10 m subplots

417   to avoid any impacts of trenching. Samples of tree stem tissue from the same trees were taken

418   with a 5 mm increment borer at breast height once in November 2013; this sampling was not

419   repeated to avoid excessive damage incurred by repeated boring. We followed the enzymatic

420   method proposed by Sevanto et al. (2014)[40] to analyze the NSC content. Here, NSC is

421   defined as free, low molecular weight sugars (glucose, fructose and sucrose) and starch.

422   Immediately after collection, samples were microwaved to stop enzymatic activity. After that,

423   samples were oven-dried at 70°C for 24–48 h and ground to fine powder. We prepared

424   approximately 12 mg of plant material with 1.6 mL of distilled water for the analysis. We

425   used amyloglucosidase from *Aspergillus niger* (Sigma-Aldrich) to digest total NSC to

426   glucose, and invertase, glucose hexokinase kits (GHK) and phosphorus glucose (Sigma-

427   Aldrich) to quantify the low molecular weight sugars. The concentration of free glucose was

428   determined photometrically in a 96-well microplate spectrophotometer (BioTek, Epoch).

429   NSC values are expressed as percent of dry matter. For further method details, see Sevanto et

430   al. (2014)[40].

431   *Xylem vulnerability to cavitation (Percentage Loss of Conductivity; PLC) and leaf water*

432   *potential measurements.* Samples were cut from fully sunlit branches following the same

433   protocol as above for NSC during late dry season (November 2013), and using the same

434   sample trees as used for the NSC analysis (Extended Data Table 1), with the exception of

435   branches of the genus *Manilkara*. To maintain a balance of number of genera and trees

436   sampled, four additional trees were therefore sampled from the genus *Inga* in the TFE and

437   control plots for both sets of analyses. One to three 1.0-1.5 m long branches per tree were cut

438   and left to rehydrate overnight under a black plastic bag in a bucket of water. Maximum

439   vessel length was determined for one branch out of a set of 5-6 branches for each species by

440   injecting low pressure air at the branch base under water and progressively re-cutting the

441   stem until bubbles emerged (maximum conduit length varied between 25 and 50 cm across

442   samples)[41]. Axial slits were made in the branch segments selected for PLC analysis to

443   increase the efficacy of the air injection. These partially debarked segments were mounted on

444   a 4.6 cm long air injection apparatus. Water, filtered to 0.2 μ, flowed gravimetrically through

445   the sample. After 10 minutes of equilibration at low pressure (10 kPa), the sample was

446   pressurised for 20 min. The pressure was increased in steps of 0.3 to 0.5 MPa, with each step

447   followed by 10 min relaxation and flow measured at a constant background 100 kPa air

448   pressure, until a residual flow lower than 5 % of the initial flow was found. Five to 10

449   measurements of water flux were taken at the distal end. The interval for each conductivity

450   measurement ranged from 2 to 10 minutes depending on stem length, conductivity and

451   pressure head employed (normally 3 kPa). Segment lengths, cross-sectional diameters and

452   leaf areas of the leaves subtended by the measured segment were determined.

453   We employed a two-parameter Weibull function to model the changes in percent loss of

454   xylem hydraulic conductivity as a function of xylem pressure[42]. The two parameters

455   represented P_{50} and slope of the conductivity-pressure curve. We estimated P_{50} and slope for

456   all trees using tree as a random factor in a mixed-model analysis (nlme library[43]) in R

457   (Version 3.02, R Core Team). We let P_{50} vary for each tree while keeping slope constant

458   across trees to achieve convergence. We then employed these conditional estimates of P_{50} in

459   a general linear model to test for the effects of plot, genus and dbh (Extended Data Table 3a).

460   We then confirmed the above results by running a second mixed-effect model, in which we

461   accounted for random tree-by-tree variation and variance driven by phylogeny, by nesting

462   individual trees within genera as the random component of the model and incorporating plot

463   and dbh as fixed effects (Extended Data Table 3b). We tested whether tree diameter affected

464   P_{50} by comparing the performance of the full model with the same model without the effect

465   of dbh on P_{50} using a likelihood ratio test, and by conducting simultaneous hypothesis tests at

466   the 95% significance level (library multcomp in R). For both analyses, distributional

467   assumptions were tested by looking at plots of residuals for fixed and, if the case, random

468   effects.

469   Leaf water potential Ψ_l was measured during two campaigns (one during the dry and one

470   during the wet season, i.e., October 2013 and May 2014, respectively). Two to four leaves

471   were measured for each branch of each tree, following the same sampling protocol above for

472   NSC and hydraulic measurements. During each campaign, Ψ_l measurements were conducted

473   at pre-dawn (prior to 07.00 hrs) and at midday (between 11.30 hrs and 1300 hr). Midday Ψ_l

474   measurements of both campaigns were used in conjunction with the P_{50} and slope values

475   determined for each genus to estimate percent loss of hydraulic conductivity (PLC), assuming

476   xylem water potential to be equal to measured leaf water potential[20]. We acknowledge that

477   this may overestimate PLC; however in counterpoint, only one seasonal campaign could be

478   conducted and so the minimum of leaf Ψ_l for that year was thus likely to have been

479   underestimated because fuller sampling through the dry season was impractical. In addition,

480   earlier (2003) studies in the same experiment[44] reported minimum values of stem xylem

481   water potentials of around -1.6 MPa, across control and TFE plots, suggesting that xylem

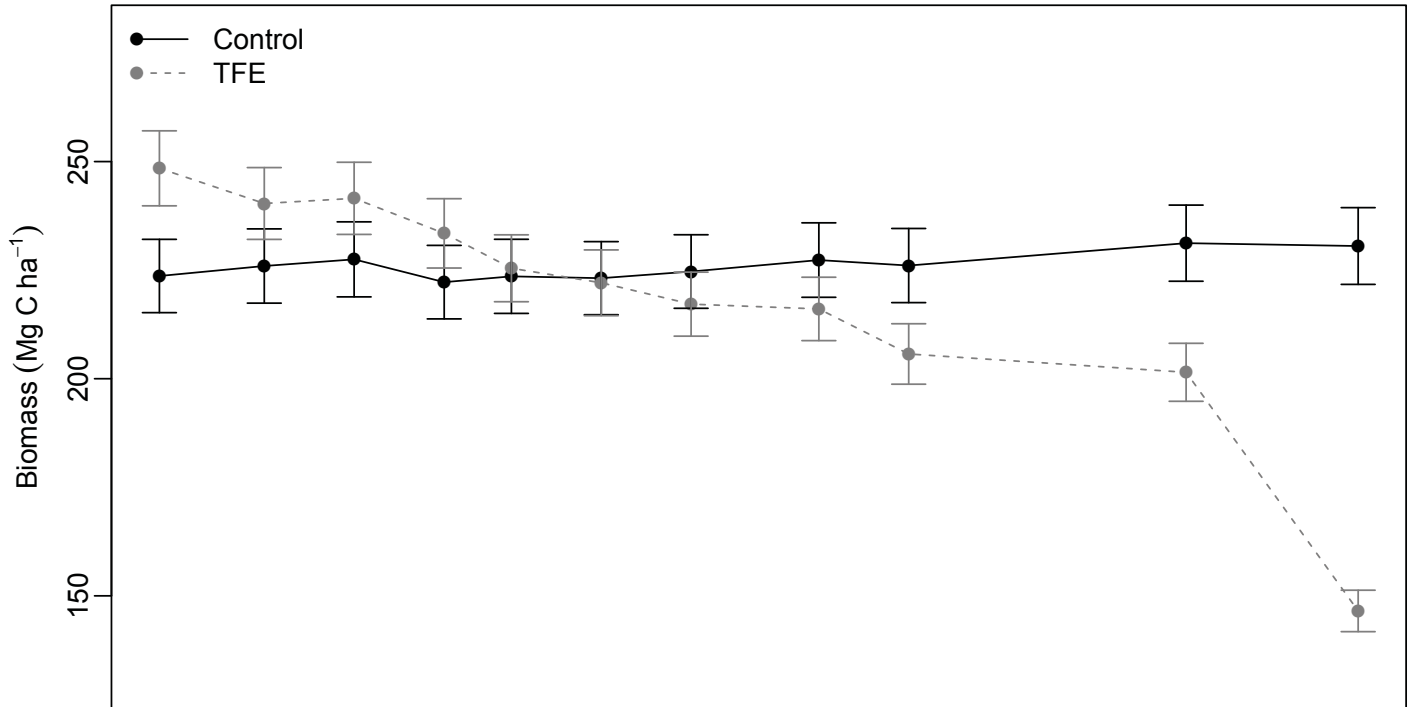482   values substantially more negative than those assumed here can be experienced.

483   *Herbivory:* All leaf material from 25 x 1 m^2 litter-traps on the control and TFE was collected

484   13 times from 2010-2014 at 3-6 month intervals, with one eight month interval in 2011. Each

485   collection of leaf material represented two weeks of litter-fall in the forest. The 9770 leaves

486   collected from all 25 per plot litter-traps over the study period were scanned and the images

487   were analysed according to Metcalfe et al.[45] to calculate the percent leaf area lost to herbivore

488   attack on the control and TFE.

489   *LAI measurements*: LAI values from 2001 to 2007 are taken from Figure 1f in Metcalfe et al.

490   (2010)[38]. For 2009-2014 LAI was measured at the same 25 permanent points[38] on a grid

491   throughout the control and TFE plot. Measurements were made using hemispherical photos

492   taken every 3-6 months from 2009-2014. Photos were taken before sunrise (~6.00 am) from a

493   height of 1.5 m on the control plot and 2 m (above the TFE structure) on the TFE plot. The 25

494   photos per plot were analysed together using the CAN_EYE software (INRA, Avignon,

495   France). Standard errors were calculated using three different estimates of LAI given by the

496   CAN_EYE software.

Extra References for Methods

29   Ruivo M & E., C. in *Ecosystems and sustainable development.*   (ed E. Tiezzi, Brebbia, C. A., Uso, J. L., (eds)) 1113–1121 (WIT Press, 2003).

30   Fisher, R. A. *et al.* The response of an Eastern Amazonian rain forest to drought stress: results and modelling analyses from a throughfall exclusion experiment. *Global Change Biol* 13, 2361-2378, doi:DOI 10.1111/j.1365-2486.2007.01417.x (2007).

31   Fisher, R. A., Williams, M., Ruivo, M. D., de Costa, A. L. & Meira, P. Evaluating climatic and soil water controls on evapotranspiration at two Amazonian rainforest sites. Agr Forest Meteorol 148, 850-861, doi:DOI 10.1016/j.agrformet.2007.12.001 (2008).

32   Chave, J. *et al.* Improved allometric models to estimate the aboveground biomass of tropical trees. *Global Change Biol* 20, 3177-3190, doi:Doi 10.1111/Gcb.12629 (2014).

33   Chave, J. *et al.* Towards a worldwide wood economics spectrum. *Ecol Lett* 12, 351-366, doi:DOI 10.1111/j.1461-0248.2009.01285.x (2009).

34   Zanne, A. E. *et al*. Data from: Towards a worldwide wood economics spectrum. Dryad Digital Repository. http://dx.doi.org/10.5061/dryad.234. (2009).

35   Patiño, S. *et al.* Branch xylem density variations across the Amazon Basin. *Biogeosciences* 6, 545-568, doi:DOI 10.5194/bg-6-545-2009 (2009).

36   Chave, J. *et al.* Tree allometry and improved estimation of carbon stocks and balance in tropical forests. *Oecologia* 145, 87-99, doi:DOI 10.1007/s00442-005-0100-x (2005).

37   Feldpausch, T. R. *et al.* Tree height integrated into pantropical forest biomass estimates. *Biogeosciences* 9, 3381-3403, doi:DOI 10.5194/bg-9-3381-2012 (2012).

522 38 Metcalfe, D. B. *et al.* Shifts in plant respiration and carbon use efficiency at a large-
523 scale drought experiment in the eastern Amazon. *New Phytol* 187, 608-621, doi:DOI
524 10.1111/j.1469-8137.2010.03319.x (2010).

525 39 Rowland, L. *et al.* The sensitivity of wood production to seasonal and interannual
526 variations in climate in a lowland Amazonian rainforest. *Oecologia* 174, 295-306,
527 doi:DOI 10.1007/s00442-013-2766-9 (2014).

528 40 Sevanto, S., McDowell, N. G., Dickman, L. T., Pangle, R. & Pockman, W. T. How do
529 trees die? A test of the hydraulic failure and carbon starvation hypotheses. *Plant Cell*
530 *Environ* 37, 153-161, doi:Doi 10.1111/Pce.12141 (2014).

531 41 Ennajeh, M., Simoes, F., Khemira, H. & Cochard, H. How reliable is the double-
532 ended pressure sleeve technique for assessing xylem vulnerability to cavitation in
533 woody angiosperms? *Physiol Plantarum* 142, 205-210, doi:DOI 10.1111/j.1399-
534 3054.2011.01470.x (2011).

535 42 Neufeld, H.S., Grantz, D.A., Meinzer, F.C., Goldstein, G., Crisosto, G.M. & Crisosto.
536 C. Genotypic variability in vulnerability of leaf xylem to cavitation in water-stressed
537 and well-irrigated sugarcane. Plant Physiol. 100:1020—1028 (1992).

538 43 Pinheiro, J. C. & Bates, D. M. *Mixed-Effects Models in S and S-PLUS.* (Springer,
539 2000).

540 44 Fisher, R. A., Williams, M., Do Vale, R. L., Da Costa, A. L. & Meir, P. Evidence
541 from Amazonian forests is consistent with isohydric control of leaf water potential.
542 *Plant Cell Environ* 29, 151-165, doi:DOI 10.1111/j.1365-3040.2005.01407.x (2006).

543 45 Metcalfe, D. B. *et al.* Herbivory makes major contributions to ecosystem carbon and
544 nutrient cycling in tropical forests. *Ecol Lett* 17, 324-332, doi:Doi 10.1111/Ele.12233
545 (2014).

a

b

a Dead Trees

b Small Trees (10−20 cm)

c Medium Trees (20−40 cm)

d Large Trees (>40cm)